Synthesis of an Alkylammonium/Magnesium Phyllosilicate Hybrid Nanocomposite Consisting of a Smectite-Like Layer and Organosiloxane Layers

Kazuko Fujii,*,† Shigenobu Hayashi,‡ and Hiroshi Kodama†

Advanced Materials Laboratory, National Institute for Materials Science, 1-1 Namiki, Tsukuba, Ibaraki 305-0044, Japan, and Institute for Materials and Chemical Process, National Institute of Advanced Industrial Science and Technology (AIST), Central 5, 1-1-1 Higashi, Tsukuba, Ibaraki 305-8565, Japan

Received September 24, 2002. Revised Manuscript Received January 14, 2003

We synthesized a novel alkylammonium/magnesium phyllosilicate hybrid compound by hydrothermal reaction from a mixture of octadecyldimethyl(3-trimethoxysilylpropyl)ammonium chloride, silica sol, and $Mg(OH)_2$. The structure of the hybrid compound was studied by XRD, TEM, electron diffraction, high-resolution solid-state NMR, TG-DTA/MS, and elemental analysis. The oscillating XRD profile indicated that the compound has a layered structure without long-range periodicity, i.e., the synthesized platelet crystal is very thin. We proposed that the compound consists of three layers, in which the central layer is a magnesium phyllosilicate analogous to trioctahedral smectites, and the sheets on both sides are siloxanes. An organic part ($C_{18}H_{37}N^+(CH_3)_2C_3H_6-$) bonds to the layers and exists between them; the hybrid compound is an assembly of a magnesium phyllo(alkylammonium)silicate part and two condensed octadecyldimethyl(3-trimethoxysilylpropyl)ammonium chloride parts; the alkylammonium chains of both parts are in an all-trans conformation and are arranged in parallel.

Introduction

Nanosheet materials have recently become subjects of special interest because of their unique structures, and their application is expected in optical and electrical fields. Some layered compounds are exfoliated in solution and changed into nanosheet materials composed of very small numbers of stacking layers.[1−3] These exfoliated thin materials are reassembled by drying, resulting in compounds with stacked layers.

Much attention has also been paid to inorganic−organic hybrid compounds.[4−16] Various compounds and methods for their synthesis have been reported. For example, these hybrid compounds have been synthesized by intercalating various organic species into two-dimensional galleries of layered materials such as smectites,[4−8] and by immobilizing organic molecules in sol−gel oxide matrixes.[9] The inorganic and organic parts do not bond covalently with each other in these compounds. Fukushima and Tani[10,11] succeeded in synthesizing inorganic−organic hybrid layered compounds by reacting organofunctional trialkoxysilanes with metal chloride hexahydrates. The hybrids have inorganic parts with phyllosilicate-like structures, such as smectites, and the organic parts of the hybrids are linked to the inorganic frameworks through Si−C covalent bonds. Parikh et al.[12] synthesized an inorganic−organic layered compound from *n*-octadecyltrichlorosilane and clarified that the organic part is linked to the inorganic part through an Si−C covalent bond, and that the organic part, which is an alkyl chain, is located between the inorganic layers. Shimojima et al.[13] reported inorganic−organic hybrid layered materials linked through Si−C covalent bonds. They synthesized these compounds by hydrolysis and polycondensation of triethoxy(alkyl)-silanes, and reported that the compounds have a bimolecular layered structure of alkyl chains between the inorganic parts. In the latter two works, the authors

* To whom correspondence should be addressed. E-mail: FUJII.Kazuko@nims.go.jp. Fax: +81-298-52-7449. Tel: +81-298-51-3354 (ext. 666 or *666).

† National Institute for Materials Science.

‡ National Institute of Advanced Industrial Science and Technology.

(1) Nadeau, P. H.; Wilson, M. J.; McHardy, W. J.; Tait, J. M. *Nature* **1984**, 923.

(2) Sasaki, T.; Watanabe, M.; Hashizume, H.; Yamada, H.; Nakazawa, H. *J. Chem. Soc., Chem. Commun.* **1996**, 229.

(3) Sasaki, T.; Watanabe, M.; Hashizume, H.; Yamada, H.; Nakazawa, H. *J. Am. Chem. Soc.* **1996**, *118*, 8329.

(4) Tamura, K.; Nakazawa, H. *Clays Clay Miner.* **1996**, *44*, 501.

(5) Fujita, T.; Iyi, N.; Klapyta, Z. *Mater. Res. Bull.* **1998**, *33*, 1693.

(6) Nunes, L. M.; Airoldi, C. *Mater. Res. Bull.* **1999**, *34*, 2121.

(7) Takagi, K.; Usami, H.; Fukaya, H.; Sawaki, Y. *J. Chem. Soc., Chem. Commun.* **1989**, 1174.

(8) Ogawa, M.; Handa, T.; Kuroda, K.; Kato, C. *Chem. Lett.* **1990**, 71.

(9) Lindner, E.; Kemmler, M.; Mayer, H. A.; Wegner, P. *J. Am. Chem. Soc.* **1994**, *116*, 348.

(10) Fukushima, Y.; Tani, M. *Bull. Chem. Soc. Jpn.* **1996**, *69*, 3667.

(11) Fukushima, Y.; Tani, M. *J. Chem. Soc., Chem. Commun.* **1995**, 241.

(12) Parikh, A. N.; Schivley, M. A.; Koo, E.; Seshadri, K.; Aurentz, D.; Mueller, K.; Allara, D. L. *J. Am. Chem. Soc.* **1997**, *119*, 3135.

(13) Shimojima, A.; Sugawara, Y.; Kuroda, K. *Bull. Chem. Soc. Jpn.* **1997**, *70*, 2847.

(14) Carrado, K. A.; Thiyagarajan, P.; Winans, R. E.; Botto, R. E. *Inorg. Chem.* **1991**, *30*, 794.

(15) da Fonseca, M. G.; Silva, C. R.; Airoldi, C. *Langmuir* **1999**, *15*, 5048. Burkett, S. L.; Press, A.; Mann, S. *Chem. Mater.* **1997**, *9*, 1071.

(16) Ruiz-Hitzky, E.; Rojo, J. M. *Nature* **1980**, *287*, 28.

10.1021/cm0209665 CCC: $25.00
Published on Web 02/13/2003

Scheme 1

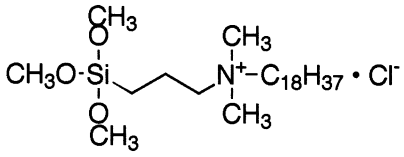

selected organosilicon compounds with long-chain (octadecyl) alkyl groups for the organic parts. The distances between layers were 5.358 nm[12] and 5.28 nm.[13] The alkyl chains between the layers were organized in an all-trans conformation, and the chain−chain spacings were 0.414 nm[12] and 0.42 nm.[13]

In the present work, we synthesize a new inorganic−organic thin layer compound and determine its structure. The synthesized material is a nanosheet material with a layered structure and without long-range periodicity. It has organic parts linked to the inorganic frameworks through Si−C covalent bonds. Octadecyldimethyl(3-trimethoxysilylpropyl)ammonium chloride (abbreviated as ODAC) was used as a starting material for the organic part. As shown in Scheme 1, this molecule contains a nitrogen atom bonded with four alkyl groups; it has a long chain and bulky side chain groups. It is presumed that the long chain promotes crystallization of the organic parts, whereas the bulky side chains disturb it. Therefore, it is very interesting to study whether this synthesis is possible and how the crystallization takes place if the synthesis is possible. There have been no reports of inorganic−organic hybrid crystals containing such kinds of organosilicon as the organic part. The inorganic part is designed to have a structure very similar to that of smectites. Silica sol and magnesium hydroxide are used as starting materials for the inorganic parts. These materials are expected to form the structure analogous to one layer of smectites, a group of clay minerals.

The synthesis is carried out by a hydrothermal method. Although this is a popular method for synthesizing inorganic materials, there are few reports that apply this method to synthesizing inorganic−organic compounds. The present work demonstrates that layered silicates bonded chemically with organic parts can be synthesized successfully by this method. The structures of the synthesized compounds were determined from various experimental results, including chemical analysis, infrared (IR) spectroscopy, X-ray diffraction (XRD) analysis, high-resolution solid-state nuclear magnetic resonance (NMR) spectroscopy, thermogravimetric and differential thermal analyses (TG-DTA), mass spectrometry (MS), and transmission electron microscope (TEM) observation.

The synthesized inorganic−organic thin layer compound has potential applications for antimicrobial materials similarly to materials treated with ODAC,[17] ion-exchange materials especially for anions, and fillers for organic polymers, among others. The synthesized compound in this study has higher potential for the fillers than intercalation compounds because it is a nanosheet material and its outermost layers are organic.

(17) Tsao, I.-Fu; Wang, H. Y.; Shipman, J. C. *Biotechnol. Bioeng.* **1989**, *34*, 639.

Experimental Section

Materials. Silica sol (Ludox HS-30) was obtained from Du Pont. $Mg(OH)_2$ was purchased from High Purity Chemicals Co. Ltd. and was also prepared by the authors from $MgCl_2 \cdot 6H_2O$ (Wako Pure Chemical Industries, Ltd.) and NH_4OH.[14] Octadecyldimethyl(3-trimethoxysilylpropyl)ammonium chloride, $C_{18}H_{37}N^+(CH_3)_2C_3H_6Si(OCH_3)_3$ (abbreviated as $C_{18}A^+$TMS or ODAC), was obtained from Toray Dow Corning Silicone Co., Ltd. and Shin-Etsu Chemical Co., Ltd.

Synthesis. Silica sol and ODAC were mixed at room temperature to form suspensions. The methoxyl groups of $C_{18}A^+$TMS are hydrolyzed by water, and the hydrolyzed $C_{18}A^+$-TMS is condensed with silanol groups. $Mg(OH)_2$ and H_2O were then added to the above suspensions under continuous stirring. After sufficient stirring, the mixtures were used as starting materials for hydrothermal synthesis. Hydrothermal reactions were carried out in a high-pressure vessel, as described previously.[18]

Characterization. XRD measurements were performed at room temperature under an ambient atmosphere and also under controlled relative humidity using Cu Kα radiation on a Rigaku Rint 2000S diffractometer equipped with a humidity/temperature controllable chamber.[19] TG-DTA/MS was carried out using a MAC Science TG-DTA/MS 2000. TEM and electron diffraction (ED) images were obtained by a Hitachi H-500. High-resolution solid-state ^{13}C and ^{29}Si NMR spectra were obtained by Bruker ASX400 and MSL400 spectrometers at room temperature. The Larmor frequencies of ^{13}C and ^{29}Si were 100.61 and 79.49 MHz, respectively. The ordinary cross polarization (CP) pulse sequence was used together with magic angle spinning (MAS) of the sample, in which the contact times were set at 1 and 5 ms for ^{13}C and ^{29}Si, respectively, and a recycle time was 6 s for both nuclei. The ordinary single pulse sequence was also used together with ^1H dipolar decoupling for the ^{29}Si measurements with a recycle time of 20 s. The samples were packed into a 7-mm rotor and the spinning rates were 4.0 kHz for ^{13}C and 4.5 kHz for ^{29}Si. The chemical shifts of both ^{13}C and ^{29}Si were referenced to neat tetramethylsilane. The IR spectra were recorded with a Bio-Rad FTS-65 FT-IR spectrometer. Elemental analysis was performed using an inductively coupled plasma (ICP) atomic absorption for magnesium and silicon and using a combustion-infrared absorption for carbon.

Results

Synthesis. Synthesis was carried out under various experimental conditions by changing the mixing ratios in the starting materials, the reaction temperatures, and the reaction times. In addition, many preliminary experiments were conducted by changing the combinations of starting materials, as various side reactions may proceed together. The temperature was tested between 150 and 250 °C. The heating time was tested between 1 and 5 days. The successful conditions were as follows: a reaction temperature of 200 °C, a reaction time of 3 days, and a molar ratio of silica sol/ODAC/$Mg(OH)_2$ of 0.76:0.76:1.00 in the starting mixture. The reaction product was filtered and dried under reduced pressure.

X-ray Diffraction. Figure 1(a) and (b) shows the XRD patterns of a reference material, smectite, and the hybrid nanocomposite successfully synthesized. The former was synthesized by a hydrothermal method from a mixture of silica sol, $Mg(OH)_2$, and LiF with a molar ratio of 1.52:1.00:0.20. All peaks in Figure 1(a) are

(18) Ueda, S. *Nendohandbook, 2nd ed. (Handbook of Clay, 2nd ed.)*; Clay Science Society of Japan, Ed.; Gihoudoushuppan Co. Ltd: Tokyo, 1987; pp 196−197.

(19) Hashizume, H.; Shimomura, S.; Yamada, H.; Fujita, T.; Nakazawa, H. *Powder Diffr.* **1996**, *11*, 288.

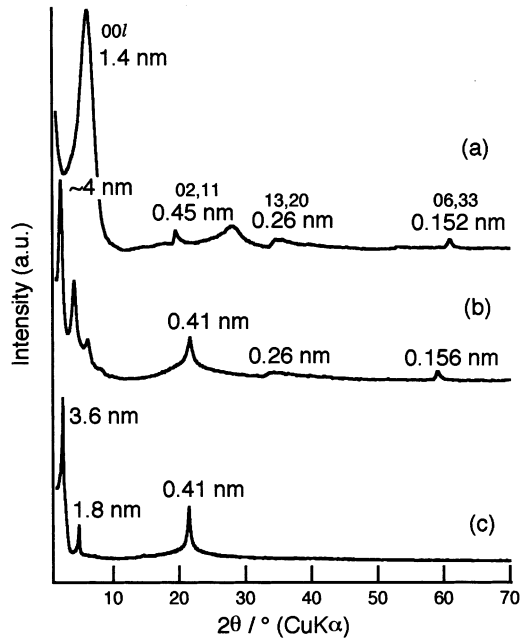

Figure 1. X-ray diffraction patterns of the reaction products obtained from starting mixtures consisting of silica sol, ODAC, $Mg(OH)_2$, and LiF with molar ratios of (a) 1.52:0:1:0.2 (a reference sample) and (b) 0.76:0.76:1:0, and (c) polycondensed ODAC.

attributed to the smectite structure. For example, the unsymmetrical peak around $2\theta = 35°$ ($d = 0.26$ nm) was indexed as 13,20[20] and the reflection peaks around $2\theta = 20°$ ($d = 0.45$ nm) and at $2\theta = 61.0°$ ($d = 0.152$ nm) were indexed as 02,11 and 06,33, respectively.[20] These results suggest that this material has the structure of typical smectites, such as stevensite and hectorite, the layers of which consist of two silicic tetrahedral sheets and an Mg octahedral sheet.

Figure 1(b) provides four pieces of important information regarding the structure of the hybrid nanocomposite. The first is that it contains an unsymmetrical peak around $2\theta = 35°$ and a reflection peak at $2\theta = 59.1°$, corresponding to $d = 0.26$ and 0.156 nm, respectively. The second is the peak observed at $2\theta = 22°$ ($d = 0.41$ nm). The third is the peak observed around $2\theta = 2.2°$ ($d = 4.0$ nm). The fourth is the characteristic oscillating profile in the low angle range ($2\theta \leq 10°$).

On the basis of the first piece of information, we can propose that the inorganic part of the hybrid nanocomposite has a structure analogous to that of smectite, although no distinct X-ray reflection peak was observed around $2\theta = 20°$ ($d = 0.45$ nm). The second piece of information allows us to propose the presence of an organized solid phase of alkyl chains, because similar peaks have been observed in crystalline *n*-alkanes[21−23] and high-surface-pressure Langmuir monolayers of hydrocarbon-chain amphiphiles,[24−28] where the *d* value (= 0.41 nm) of the peaks was explained as corresponding to the spacing between the alkyl chains. A crystalline polymer was obtained as a reference material in the present study by polycondensation of ODAC, the XRD of which had a peak corresponding to $d = 0.41$ nm (shown in Figure 1(c)). The reflection was caused by a crystalline assembly of alkyl chains. The third piece of information suggests that the spacing between the layers is around 4.0 nm. The 4.0-nm space is large enough to accommodate the organic chains.

The fourth piece of information will be discussed in detail. It has been reported in studies of a nanosheet, such as exfoliated titanate,[2,3] that its XRD pattern, in a low angle range corresponding to long spacings (2.8−5.5 nm), is characterized by a wavy variation of the intensity without a flat region between the peaks, i.e., an oscillating XRD profile. This profile implies that a very small number of sheets participate in the diffraction. The intensity of the XRD pattern can be approximated by the equation described below.[2,3]

$$I(\theta) = \frac{1 + \cos^2 2\theta}{\sin^2\theta \cos\theta} \times F^2(\theta) \times \frac{\sin^2(2\pi N d \sin\theta/\lambda)}{\sin^2(2\pi d \sin\theta/\lambda)}$$

The first term is a Lorentz-polarization factor, the second is a structure factor, and the third is an interference function. θ is the scattering angle, d is the spacing, λ is the wavelength of the incident X-ray, and N is the number of periodic sheets that participate in the reflection. When N is less than 8, the third term oscillates as a function of θ. For example, the XRD patterns of ultrathin materials such as exfoliated clays[1] and titanate[2,3] exhibit oscillating profiles. Therefore, the oscillating XRD pattern of layered compounds suggests that there are very few sheets stacked in one crystallite. These oscillating XRD profiles were observed in the present study, as shown in Figure 1(b). However, there is also the possibility that a pattern with a rational series of reflections for a compound stacked with many well-ordered sheets is overlapped with the direct beam of the scattering X-ray. The pattern might be strongly influenced by the direct beam of the scattering X-ray, considering it was observed in a very low angle range.

The XRDs were measured for solids suspended in aqueous solutions in order to ascertain the origin of the observed profile. The suspension was set under a constant humidity during the measurements, and the humidity was changed from 95% to 6% in 10 steps. More specifically, the liquid was evaporated through 10 steps, and at the final step the solids in the suspension formed a film on the surface of a glass plate. Figure 2 shows the XRD patterns under different levels of relative humidity. A difference in the "degree of dryness" yields different numbers of crystals in the unit volume of the suspensions and different conditions for the orientation and dispersion of the crystals. As shown in Figure 2, the intensity of the diffraction peaks increased with a decrease in the relative humidity. This is caused by the change described above. Four wavy variations were

(20) Brindley, G. W. *Crystal Structures of Clay Minerals And Their X-ray Identification*; Brindley, G. W., Brown, G., Eds.; Mineralogical Society: London, 1980.
(21) Unger, G. *J. Phys. Chem.* **1983**, *87*, 689.
(22) Doucet, J.; Denicolo, I.; Craievich, A.; Collet, A. *J. Chem. Phys.* **1981**, *75*, 5125.
(23) Ewen, B.; Strobl, G. R.; Richter, D. *Faraday Discuss.* **1980**, *69*, 19.
(24) Barton, S. W.; Thomas, B. N.; Flom, E. B.; Rice, S. A.; Lin, B.; Ketterson, J. B.; Dutta, P. *J. Chem. Phys.* **1988**, *89*, 2257.
(25) Kjaer, K.; Als-Nielsen, J.; Helm, C. A.; Laxhauber, L. A.; Mohwald, H. *Phys. Rev. Lett.* **1987**, *158*, 2224.
(26) Helm, C. A.; Mohwals, H.; Kajaer, K.; Als-Nielsen, J. *Biophys. J.* **1987**, *52*, 381.
(27) Barton, S. W.; Thomas, B. N.; Flom, E. B.; Novak, F.; Rice, S. A. *Langmuir* **1988**, *4*, 233.
(28) Tippman-Krayer, P.; Mohwald, H. *Langmuir* **1991**, *7*, 2303.

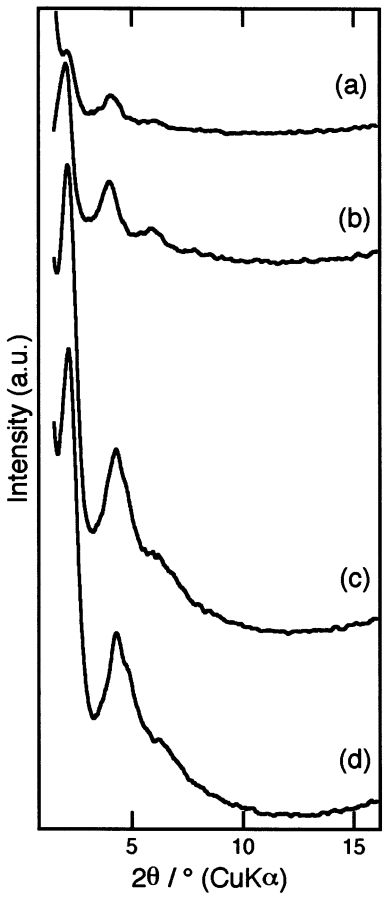

Figure 2. XRD patterns of the hybrid nanocomposite equilibrated with various levels of humidity at 30 °C. The relative humidity was (a) 90%, (b) 70%, (c) 50%, and (d) 30%.

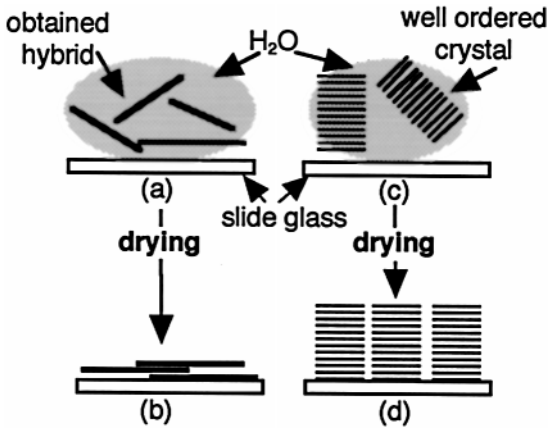

Figure 3. Schematic drawing of the orientation and the dispersion of the compound; a very small number of stacking layers (a and b) and crystals with high regularity (c and d). Parts (a) and (c) represent the sheets in the starting suspensions; (b) and (d) represent the sheets after drying.

observed in the XRD profiles, as shown in Figure 2(a) and (b). However, the third peak became vague, and no fourth peak was observed, as seen in Figure 2(c) and (d). This change can be explained by the model shown in Figure 3(a) and (b), not by Figure 3(c) and (d). The crystals were suspended in the relative humidity steps of 90% and 70%, as shown in Figure 3(a). Most of the crystals were stacked as layers parallel to the glass plate in relative humidity steps of 50% and 30%, as shown in Figure 3(b), because the crystal habit is a thin platelet, which is clarified by TEM observation in the next section. In contrast, if the crystals suspended in water consisted of many well-ordered sheets, as shown schematically in Figure 3(c), the observed change would not be expected in the XRD profile before and after drying.

In conclusion, the characteristic oscillating XRD profile in Figure 1(b) demonstrates that a very small number of sheets participate in the diffraction; thus, the hybrid nanocomposite is an ultrathin layered compound.

TEM Image. Figure 4 shows a TEM image of the hybrid nanocomposite, which exhibits a platelet habit. The inset in Figure 4 shows an electron diffraction pattern. The *d* values of the diffraction spots agree with the XRD pattern (Figure 1(b)). In addition, the directions of the diffraction spots are compatible with the smectite-like structure proposed in the previous section.

^{13}C NMR. The structure of the organic part was studied by means of high-resolution solid-state ^{13}C NMR and IR. Figure 5(a) shows a ^{13}C CP/MAS NMR spectrum of the hybrid nanocomposite. Figure 5(b) shows the spectrum of the reference material, ODAC dissolved in methanol, which was used for peak assignments. All the peaks in Figure 5(a) were assigned to carbons in the chemical formula in Figure 5. The carbons at chain positions 1−10, except for 3 and 5, were confirmed for the hybrid nanocomposite as well as the polycondensed ODAC (PODAC). The assignment of the carbon at position 5 was not established, even for the reference material. Although a ^{13}C NMR peak corresponding to the CH_3O species was observed at 50 ppm for ODAC in methanol, the peak was not observed for the hybrid nanocomposite or PODAC. This suggests that the methoxyl groups were hydrolyzed and that the condensation reaction proceeded, leading to the formation of Si−O−Si linkages. Consequently, the organic part in the hybrid nanocomposite is $C_{18}H_{37}N^+(CH_3)_2C_3H_6Si$.

The ^{13}C chemical shift reflects the molecular conformations.[29] The ^{13}C chemical shifts were about 33 ppm for crystalline compounds with an all-trans zigzag conformation, such as crystallized polyethylene,[30] *n*-paraffin (orthorhombic form), and the layered crystalline polymer.[12] In contrast, it was about 31 ppm when alkyl chains formed a noncrystalline region in polyethylene.[31] The ^{13}C NMR spectrum of the hybrid nanocomposite exhibits two ^{13}C NMR peaks that correspond to the carbon at position 4. The most intense peak at 33 ppm indicates high populations of the trans conformation in the alkyl chains, while the peak at 31 ppm shows the presence of the gauche−trans conformation. Conclusively, the majority of the organic parts are packed with the all-trans conformation, though organic parts packed with the gauche−trans conformation also exist.

^{29}Si NMR. The hybrid nanocomposite consists of an inorganic part and an organic part; the former has a magnesium phyllosilicate structure and the latter is $C_{18}H_{37}N^+(CH_3)_2C_3H_6Si$. Information of the chemical bonds between the two parts can be obtained from high-resolution solid-state ^{29}Si NMR spectra, which are shown in Figure 6(a) and (b).

(29) Yamanobe, T.; Sorita, T.; Komoto, T.; Ando, I.; Sato, H. *J. Mol. Struct.* **1985**, *131*, 267.
(30) Ando, I.; Sorita, T.; Yamanobe, T.; Komoto, T.; Sato, H.; Deguchi, K.; Imanari, M. *Polymer* **1985**, *26*, 1864.
(31) Earl, W. L.; VanderHart, D. L. *Macromolecules* **1979**, *12*, 762.

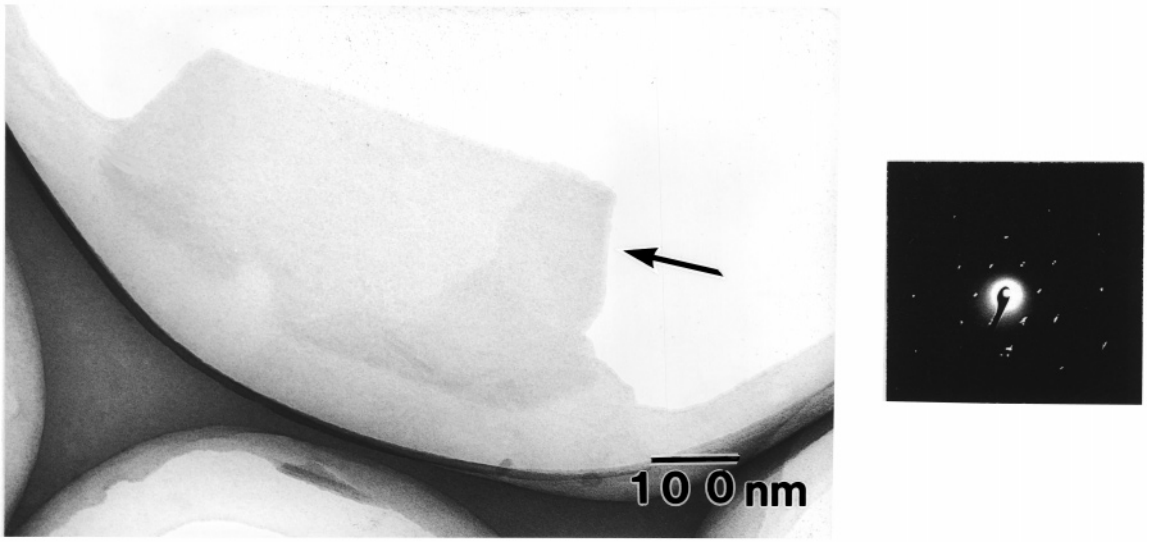

Figure 4. TEM image of the hybrid nanocomposite, with its electron diffraction pattern in the inset. The arrow indicates the platelet habit of the hybrid nanocomposite.

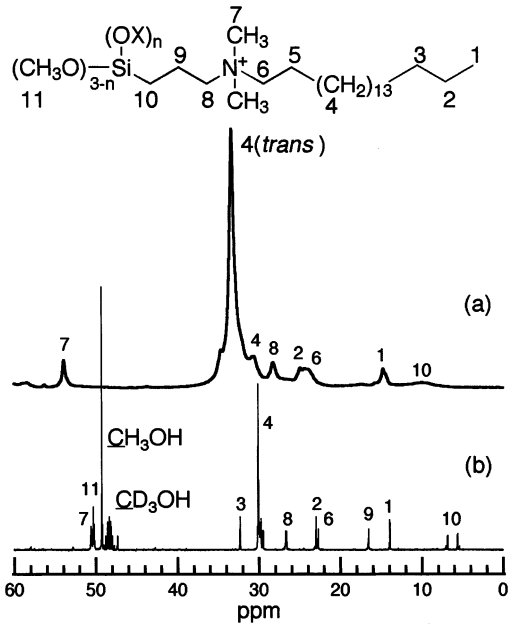

Figure 5. (a) ^{13}C CP/MAS NMR spectrum of the hybrid nanocomposite, and (b) ^{13}C NMR spectrum of ODAC dissolved in methyl alcohol.

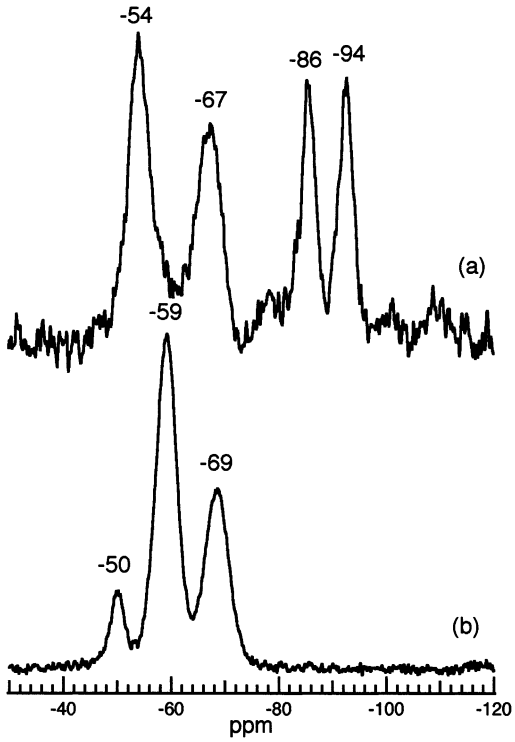

Figure 6. ^{29}Si CP/MAS NMR spectra of (a) the hybrid nanocomposite and (b) PODAC as a reference.

In this paper, the environments of silicon atoms are represented using the number of siloxane bonds, according to convention. $Si(OMg)(OSi)_k(OX)_{3-k}$ (X is H or CH_3) is then a silicon atom species with an Si−O−Mg bond, Si−O−Si bonds, and Si−O−X bonds, and is represented as Q_k'. Species with a C−Si bond, $CSi(OSi)_m(OX)_{3-m}$ and $CSi(OMg)(OSi)_n(OX)_{2-n}$, are expressed as T^m and T_n', respectively. Signals from Q type Si atoms appear in the region of −80 to −120 ppm and signals from T type Si atoms appear at −40 to −80 ppm.[32,33] Fukushima and Tani[10,11] reported that signals of T_0', T_1', and T_2' appeared at about −50, −58, and −68 ppm, respectively. Shimojima et al.[13] reported that signals of T^1, T^2, and T^3 appeared at around −48, −57 and −68 ppm, respectively.

Two signals were observed in the Q-type Si region, and two signals were observed in the T-type Si region for the hybrid nanocomposite in the present work, as shown in Figure 6(a). In contrast, three signals appeared in the T-type Si region for PODAC, as shown in Figure 6(b). The ^{29}Si NMR spectrum of ODAC solved in methanol had a signal around −44 ppm, which was assigned to T^0 (the spectrum is not shown here). Therefore, the signals at −50, −59, and −69 ppm in Figure 6(b) can be assigned to T^1, T^2, and T^3, respectively.

The peaks in the T-type Si region of the hybrid nanocomposite (Figure 6(a)) can be assigned to T_n' ($CSi(OMg)(OSi)_n(OH)_{2-n}$) and/or T^m ($CSi(OSi)_m(OH)_{3-m}$, $m \geq 1$). This suggests that a part of the Si atoms that

(32) Maxka, J.; Adams, B. R.; West, R. *J. Am. Chem. Soc.* **1989**, *111*, 3447.
(33) Slada, R. C. T.; Davis, T. N. *Colloids Surf.* **1989**, *36*, 119.

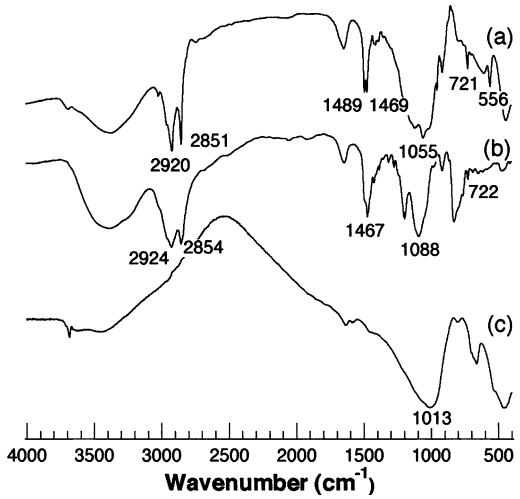

Figure 7. IR spectra of (a) the hybrid nanocomposite, (b) ODAC, and (c) smectite.

form the Si−O−Si network in the inorganic part are bonded with the organic part through Si−C covalent bonds. This agrees with the results of the ^{13}C NMR spectra.

The chemical shift of −94 ppm in Figure 6(a) is in agreement with that for the Q_3' silicon of hectorite, (Si(OMg)(OSi)$_3$), which is a kind of clay mineral with a magnesium phyllosilicate structure.[34] The presence of the magnesium phyllosilicate-like structure was also suggested by the XRD results described above. Another signal at −86 ppm can be assigned to Q_2' (Si(OMg)-(OSi)$_2$(OH)). The intensity ratio of the peak at −86 ppm to that at −94 ppm was very high in comparison with that for hectorite, even in the ^{29}Si NMR spectra measured with the single pulse sequence. T-type Si invariably produces Q_2' in a magnesium phyllosilicate structure. Therefore, this high ratio is consistent with the existence of T-type Si.

Infrared Spectroscopy. IR spectra were obtained for three samples: the hybrid nanocomposite, ODAC in methyl alcohol, and smectite, and are given in Figure 7(a), (b), and (c). The spectra in Figure 7(a) and (b) show four peaks around 2920, 2850, 1470, and 720 cm^{-1}, which are assigned to antisymmetric and symmetric stretching vibrations of the alkyl chains, a CH_2 scissoring deformation mode, and a CH_2 rocking mode, respectively. Therefore, the IR spectrum in Figure 7(a) indicates the presence of the alkyl chains in the hybrid nanocomposite.

Moreover, broad peaks observed around 1000 cm^{-1} in Figure 7(a) were assigned to Si−O−Si stretching vibrations. The characteristics of those peaks differed from those in smectite (Figure 7(c)). This suggests that the Si−O−Si linkages in the hybrid nanocomposite are not identical to those in smectite. The peaks around 550 cm^{-1} in Figure 7(a) and (c) were assigned to the Mg−O vibration band; this supports the presence of a smectite-like structure in the hybrid nanocomposite.

The full widths at half-maximum (fwhm) of the CH_2 absorption peaks around 2920, 2850, and 1470 cm^{-1} provide information regarding crystalline chain packing, i.e., the trans or gauche−trans conformation of alkyl chains. Sharp peaks with fwhm less than 15 cm^{-1} indicate a highly crystallized trans conformation of the alkyl chains. However, the peaks of the hybrid nanocomposite are not narrow (fwhm larger than 15 cm^{-1}), probably because of an overlapping of the peaks that originated from the trans and gauche−trans conformations of the alkyl chains. The presence of these two conformations was also confirmed by ^{13}C NMR.

(34) Hayashi, S. unpublished data measured for hectorite.

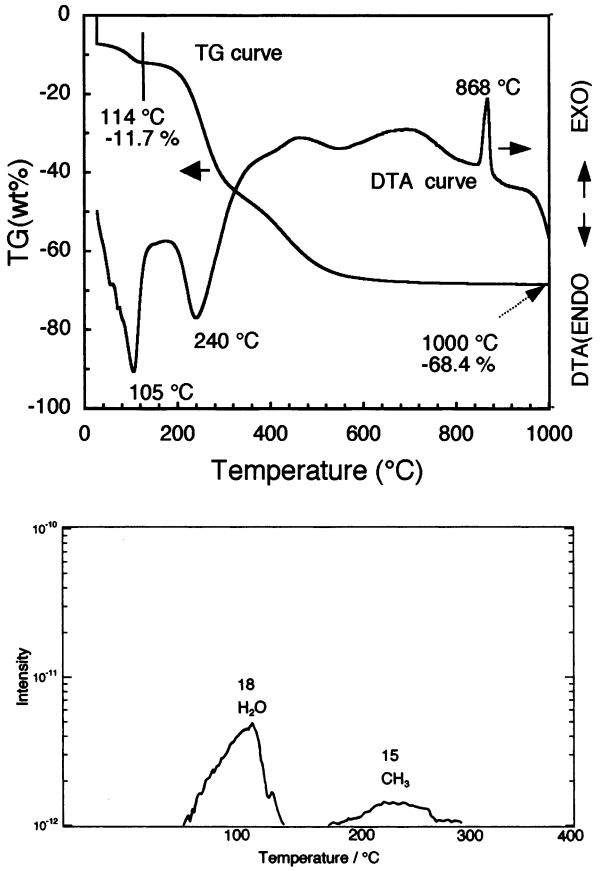

Figure 8. (a) TG-DTA curves and (b) mass spectra in an Ar gas flow for the hybrid nanocomposite. The initial mass was measured, and then the sample was kept in the Ar flow for several hours at room temperature before the temperature started to rise.

Elemental Analysis and TG-DTA/MS. An elemental analysis of the hybrid nanocomposite yielded the results C, 39.5; Mg, 5.4; Si, 9.9%; corresponding-to-molar ratios of 14.8:1.00:1.59. The final residual weight after perfect thermal decomposition is predicted to be 30.2% if a mixture of SiO_2 and MgO or their reacted compounds remain.

The thermal decomposition was studied by TG-DTA and MS, as shown in Figures 8 and 9. The TG curve in Figure 8(a) was observed in an Ar gas flow and indicates two regions of mass loss. The first one, observed between room temperature and 114 °C, was caused by a release of water within the siloxy network, which was confirmed by MS, as shown in Figure 8(b). About 11.7% of water was involved in the sample. The second region, observed above 200 °C, was caused by decomposition of the organic part. MS confirmed a CH_3 fragment, as shown in Figure 8(b). The DTA curve in Figure 8(a) demonstrates that the decompositions are endothermic reactions.

Figure 9 shows the TG-DTA curves obtained in an O_2 gas flow. The mass loss ended at about 830 °C, and

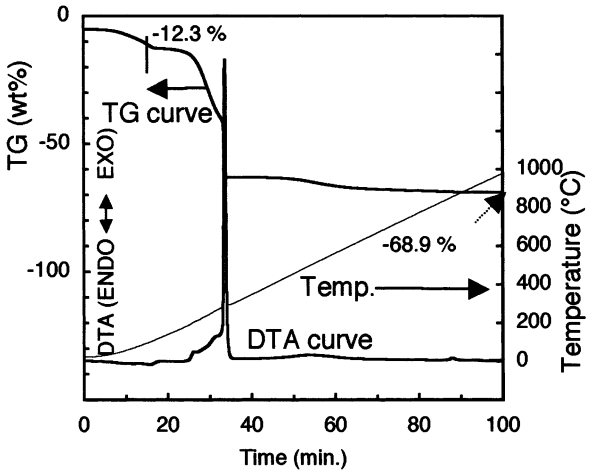

Figure 9. TG-DTA curves in an O_2 gas flow for the hybrid nanocomposite. The initial mass was measured, and then the sample was kept in the O_2 flow for several hours at room temperature before the temperature started to rise.

the final mass loss was 68.9%. The final residual weight of 31.1% agrees with the above value predicted for the residual weight after the perfect thermal decomposition from the elemental analysis.

Washing Effects. The effect of methanol washing was examined to clarify the structure of the hybrid nanocomposite. The nanocomposite was put in methanol. After sufficient stirring, the solid product was separated by filtration and dried. At the same time, the alcohol solution separated after filtration was evaporated, and the materials dissolved in it were collected. These two materials, the washed hybrid nanocomposite and the residue after evaporation, were characterized by the methods described in the previous sections.

Elemental analysis of the washed hybrid nanocomposite yielded the following results: C, 21.0; Mg, 13.6; Si, 17.3%. The final mass loss after perfect thermal decomposition of the washed hybrid nanocomposite was calculated to be 40.4% by using the results of the elemental analysis. The experimental value was 41.4%, which was obtained by a TG analysis in the O_2 gas flow. The molar ratios of C/Mg/Si of the hybrid nanocomposite were 14.8:1.00:1.59 and 3.12:1.00:1.10, before and after washing, respectively. The ratios of Si and C to Mg decreased after washing. For reference, more than 1 g of PODAC dissolves into 100 g of alcohol. These results suggest that the hybrid nanocomposite contains a PODAC-like component.

The IR peaks of the washed hybrid nanocomposite were assigned to the same alkyl group as those in the unwashed one, although the intensities of the absorption peaks were weaker than those of the unwashed sample. The absorption peak around 1055 cm^{-1} became smaller or disappeared in the washing. The peaks in the region 1090−1020 cm^{-1} were assigned to the Si−O−Si or Si−O−C bonds. In contrast, the IR spectrum of the residue had absorption peaks assigned to the alkyl group and a peak around 1055 cm^{-1}. These facts demonstrate that the Si−O−Si or Si−O−C bonds that disappeared from the washed sample were involved in the residue. In conclusion, the IR results indicate that condensed ODAC was eluted from the hybrid nanocomposite by alcohol washing.

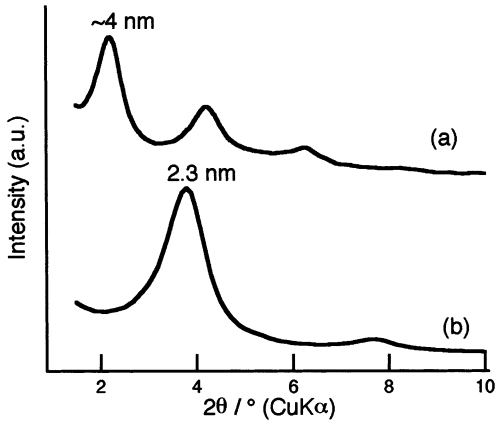

Figure 10. X-ray diffraction patterns of the hybrid nanocomposite (a) before and (b) after washing in methyl alcohol.

Figure 10 shows XRD patterns of the unwashed hybrid nanocomposite and the washed one. The peak at the lowest 2θ was shifted from 2.2° to 3.8° by washing. This result suggests that the spacing between the layers was decreased from 4.0 to 2.3 nm. Considering 2.3 nm is shorter than the full length of the organic chain, the alkyl chains are slanted from normal to the layers. Similar experimental results were obtained when the hybrid nanocomposite was washed with propyl alcohol, which dissolves PODAC. In contrast, there was no change before and after washing with benzene and hexane, which hardly dissolve PODAC.

Discussion

Structure Model of the Hybrid Nanocomposite. The wide variety of characterization data presented in the earlier sections led to a conclusion that the hybrid nanocomposite consists of an inorganic part, a magnesium phyllosilicate layer with a structure analogous to that of smectites, and an organic part of octadecyl(3-silylpropyl)dimethylammonium ($C_{18}H_{37}N^+(CH_3)_2C_3H_6-$). XRD and ^{13}C NMR also confirmed that the majority of the alkyl chains are organized in an all-trans conformation and that the chain−chain spacing is about 0.41 nm. Furthermore, we demonstrated that the inorganic part is bonded with the organic part through the Si−C covalent bond.

The above information led to the structure unit model shown in Figure 11(a), which consists of a 2:1 trioctahedral phyllosilicate part and an alkylammonium part grafted to the Mg phyllosilicate part through the Si−C bond. The structure unit is referred to as the phyllo(alkylammonium)silicate part in this paper. A periodic layered structure model (Figure 11(b)) may be proposed by stacking the structure unit shown in Figure 11(a) for the hybrid nanocomposite from the analogy with the structure described for layered inorganic/organic hybrids.[10−13,15] It consists of only smectite-like layers that sandwich alkyl chains. However, this model is unacceptable for the following reasons. In this model, the inorganic layers can repeat periodically over a long range, although the XRD results demonstrated a lack of long-range periodicity. The basal spacing expected for a model with a bimolecular structure of the alkyl chains is about 7 nm, which is inconsistent with the observed *d* value of 4 nm. Furthermore, the model in Figure 11-

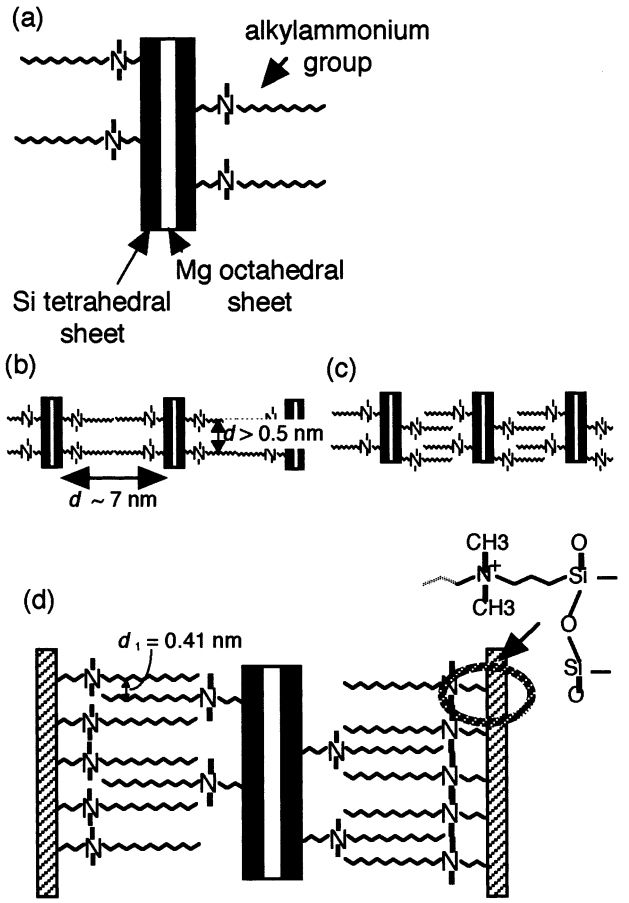

Figure 11. Schematic representation of the structure models: (a) a magnesium phyllo(alkylammonium)silicate unit; (b) the simple stacking structure of (a); (c) the stacking structure of (a) with alternatively organized alkyl chains; and (d) the proposed structure model for the hybrid nanocomposite.

(b) cannot satisfy the organization of alkyl chains between the layers described above. The spacing between the alkyl chains on the same inorganic layer should be greater than 0.5 nm because of the bulky dimethylammonium group. The XRD results indicated that the chain−chain spacing is 0.41 nm.

If the alkyl chains of the phyllo(alkylammonium)-silicate unit are arranged alternately, as shown in Figure 11(c), the interplanar spacing seems to decrease to a suitable value and the chain−chain spacing decreases. However, the structure model in Figure 11(c) cannot explain the lack of long-range periodicity or the washing effects.

The results of washing with alcohol revealed the existence of condensed ODAC. The hybrid nanocomposite is composed of the condensed ODAC and the phyllo-(alkylammonium)silicate part. We propose the structure model shown in Figure 11(d), in which the alkyl chains of both parts are inserted alternately. The structure is constructed of three layers. The central one is the inorganic layer containing two silicic tetrahedral sheets and a magnesium octahedral sheet. The outermost layers are the organosiloxane sheets containing Si−O−Si networks. The organic parts are held between two inorganic layers through Si−C covalent bonds. The alkyl chains can take a chain−chain spacing of about 0.41 nm with the all-trans conformation. The basal spacing for this structure model is estimated as follows. A fully

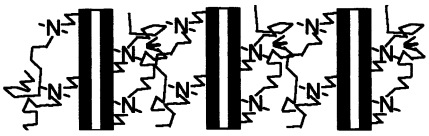

Figure 12. Schematic representation of the structure model for the hybrid nanocomposite after washing.

extended chain length of $C_{18}H_{37}N^+(CH_3)_2(CH_2)_3Si-O$ is about 3.20 nm, being estimated by reference to a chain length of $C_{18}H_{37}Si-O$[12] in the calculation of a length of C−Si−O. The literature[35] designates 0.66 nm for the thickness of one layer of typical smectites consisting of two Si tetrahedral sheets and one cation octahedral sheet. Therefore, 0.33 nm contributes to the basal spacing. A part of the organic chain, $N^+(CH_2)_3-Si$, is considered to contribute to the basal spacing, the length of which is 0.40 nm. The sum of these distances is then 3.93 nm, which agrees with the interplanar distance of 4.0 nm in the XRD results. The outermost layers are organosiloxane sheets, which may be the reason that there is no long-range periodicity for the hybrid nanocomposite. Thus, the model in Figure 11(d) is consistent with all the experimental results.

The above structure has two unique characteristics. The first is that the layered unit does not make any continuous periodic structure. The second is that the organic part is sandwiched by two different kinds of layers, the smectite-like layer and a sheet consisting of Si, O, and OH.

The formation mechanism is tentatively proposed as follows. The hydrophobic nature of the long alkyl chain causes an aggregation of ODAC in the aqua media, and the ammonium and trimethoxysilane groups of ODAC are then located outside of the hydrophobic region. Reaction of the trimethoxysilane groups with silica sol and $Mg(OH)_2$ forms the Mg phyllosilicate structure. Finally, the outermost layers of the organosiloxane sheets are formed by condensation of the trimethoxysilane groups.

Washing Effect and Chemical Formula of the Hybrid Nanocomposite. In this section, we discuss the washing effect, based on the structure model shown in Figure 11(d). When the hybrid nanocomposite is put into alcohol, the outermost layers of the organosiloxane part dissolve because polycondensed ODAC dissolves in alcohol. The phyllo(alkylammonium)silicate part shown in Figure 11(a) remains undissolved, and it forms the layered compound schematically shown in Figure 12 after drying. Because of the low density of the alkyl chains on the layer surface, the alkyl chains are no longer organized in an all-trans conformation and have gauche−trans populations. They are slanted from the normal to the layers. The observed *d* spacing of 2.3 nm supports this structure.

As described in the Results section, the molar ratios of C/Mg/Si were 14.8:1.00:1.59 (= 44:3.0:4.8) and 3.12:1.00:1.10 (= 9.4:3.0:3.3) before and after washing with alcohol, respectively. On the basis of the elemental analysis results and the structure models in Figure 11-(d) and Figure 12, the hybrid nanocomposite can be expressed as $R_{1.9}Si_{4.8}Mg_{3.0}O_p(OH)_q$ and $R_{0.41}Si_{3.3}Mg_{3.0}O_{p'}$-

(35) Moore, D. M.; Reynolds, R. C., Jr. *X-ray Diffraction and the Identification and Analysis of Clay Minerals, Second edition*; Oxford University Press: New York, 1997; pp 96−102.

$(OH)_{q'}$ before and after washing, respectively. R is the organic part, $C_{18}H_{37}N^{+}(CH_3)_2(CH_2)_3-$, which contains 23 carbons. The first formula can also be represented as $R_{(0.4+1.5)}$ $Si_{(3.3+1.5)}Mg_{3.0}O_p(OH)_q$, which suggests elution of condensed ODAC from the hybrid nanocomposite into alcohol.

Defects in the Phyllo(alkylammonium)silicate Part. The composition of the phyllo(alkylammonium)-silicate part is $R_{0.41}Si_{3.3}Mg_{3.0}O_{p'}(OH)_{q'}$, as described in the previous section. It suggests the presence of defects in the Si tetrahedral sheet. The defects are produced by Si atoms with the Si−C covalent bond in the tetrahedral sheet. In the case of layered phyllosilicates such as mica and smectite, silicon tetrahedra are linked with neighboring tetrahedra by sharing three corners (the basal oxygen) to form a hexagonal mesh pattern and with the adjacent octahedral sheet by sharing one corner (the apical oxygen).[20] In contrast, only three corners are shared with the neighboring tetrahedra and the adjacent octahedral sheet when the Si atom with the Si−C bond is located in the Si tetrahedral site. Therefore, the hexagonal mesh pattern is not formed completely, and there are defects bearing OH groups.

The existence of defects is reflected in the XRD result in Figure 1(b). The 06 band is observed at $2\theta = 59.1°$ and the corresponding d value reflects the lateral dimension, that is, an axial repeat along a line connecting the centers of neighboring SiO_4 tetrahedra or neighboring octahedra. The d value of the 06 band is usually used for identifications of the clay minerals such as the smectites and chlorites. The lateral dimensions in free states differ between the octahedral and the tetrahedral sheets. The ideal dimension for a Mg trioctahedral sheet corresponds to $d = 0.156$ nm in the free state, which is estimated by reference to the lateral dimension of brucite. In contrast, the ideal dimension for a Si tetrahedral sheet corresponds to $d = 0.153 \pm 0.001$ nm in the free state, which is calculated assuming $Si-O = 0.1618 \pm 0.001$ nm and a hexagonal geometry. If the octahedral and the tetrahedral sheets were articulated into one layer, the lateral dimensions would be adjusted to eliminate the above misfit.[20] In fact, the d values are 0.153 and 0.152 nm for the 06 bands of hectorite and stevensite, respectively. They are classified into trioctahedral smectite, and hexagonal mesh patterns are formed. However, an X-ray reflection peak was observed at 59.1° that corresponded to a d value of 0.156 nm for the hybrid nanocomposite. This d value is in agreement with the ideal dimension of the octahedral sheet. This indicates that there are so many defects in the tetrahedral sheet that the hexagonal mesh pattern is not formed. Consequently, the Mg trioctahedral sheet supports the structure of the hybrid nanocomposite. The all-trans conformation of the long alkyl chains also supports the structure in the same manner as in the layered inorganic/organic hybrids.[10,11,15]

Conclusions

We synthesized an alkylammonium/magnesium phyllosilicate hybrid nanocomposite and proposed the structure model shown in Figure 11(d) and the chemical formula $R_{(0.4+1.5)}Si_{(3.3+1.5)}Mg_{3.0}O_p(OH)_q$, where R is organic parts ($C_{18}H_{37}N^{+}(CH_3)_2C_3H_6-$), on the basis of experimental observations. The nanocomposite consists of three layers in which the central layer is magnesium phyllosilicate analogous to a 2:1 trioctahedral phyllosilicate structure, and the sheets on both sides are siloxanes. These layers do not have any periodic repeats over a long range. The organic parts are sandwiched between different kinds of layers and are bonded to the layers through Si−C covalent bonds. Because the alkyl chain has side chains, the alkyl chains take a monomolecular structure with an all-trans conformation. Thus, the synthesized material has a very novel structure.

Acknowledgment. We are grateful to Y. Yajima and S. Takenouchi, NIMS, for elemental analyses; to Y. Kitami, NIMS, for the TEM observation; and to H. Hashizume, NIMS, for the XRD measurements.

CM0209665